POLITECNICO
MILANO 1863

SCUOLA DI INGEGNERIA INDUSTRIALE
E DELL'INFORMAZIONE

Executive Summary of the Thesis

Study of Suprathermal Electron Dynamics by Modelling the Electron Cyclotron Emission

Laurea Magistrale in Nuclear Engineering - Ingegneria Nucleare

Author: Lorenzo Votta

Advisor: Prof. David Dellasega

Co-advisors: Joan Decker, Mathias Hoppe

Academic year: 2021-2022

1. Introduction

In a global context plagued by climate change and the ever-increasing demand for energy, the use of nuclear fusion as an abundant and renewable energy source is of primary importance. Among the various concepts developed to exploit the nuclear fusion reaction between deuterium and tritium, so-called magnetic confinement fusion (MCF) of a hot thermonuclear plasma is the most studied and promising technology for future energy production. Tokamaks are one of toroidal machines capable of confining plasma by means of magnetic fields. These magnetic fields are of three types: an externally induced toroidal and vertical field and a poloidal field generated by the plasma itself. The first, generated using toroidal coils, generates a direct field around the axis of symmetry of the torus that constrains the charged particles to flow along that direction. The second, generated by means of coils, allows the position of the plasma within the torus to be controlled. The third, ensures plasma equilibrium. Globally, the tokamak equilibrium magnetic field scales radially as $\boldsymbol{B}_0 \propto 1/R$, where R is the major radius. By means of the magnetic field, it is possible to distinguish two sections in a tokamak: the high field side (HFS) where the magnetic field strength is higher with respect to the other section, the low field side (LFS). Among all the tokamaks, the *Tokamak à Configuration Variable* (TCV) - hosted at EPFL in Lausanne - produced the experimental data used in this thesis. In certain scenarios, a tokamak plasma may contain a significant proportion of suprathermal particles whose energy exceeds that of the thermal particles by several orders of magnitude, affecting both temperature measurements and profile reconstruction. In particular, suprathermal electrons can play different roles. For example, in electron cyclotron current drive (ECCD) scenarios, they are beneficial since they carry the plasma current, while in presence of highly energetic runaway electrons (REs) they are dangerous for the machine integrity. Modelling the suprathermal electron dynamics in tokamaks constitute one of the main challenges in MCF.

1.1. Thesis Objectives

Electrons gyrating around magnetic field lines emit radiation at the frequency $\Omega_c = n\,eB/(\gamma m_e)$, where e is the elementary charge, B is the magnetic field amplitude, m_e is the electron rest mass, γ is the ralativistic factor

and n is the harmonic number. This radiation mechanism is called electron cyclotron emission (ECE). The ECE is a polarized emission, in fact it is possible to distinguish an Ordinary mode ($\boldsymbol{E} \parallel \boldsymbol{B}_0$) and an eXtraordinary mode ($\boldsymbol{E} \perp \boldsymbol{B}_0$). In the presence of a magnetic field amplitude gradient, as in a tokamak, the origin of emission is related to the frequency of the emission and a temperature profile can be reconstructed by scanning a range of frequencies, which is the general purpose of ECE diagnostics. Reconstructing the 3D bounce-averaged electron distribution function from ECE measurements, in non-thermal scenarios, is an ill-conditioned problem and a more promising approach consists of constructing an equivalent synthetic ECE diagnostic providing simulations that can be directly compared to measurements. Therefore, in this thesis, a new general synthetic ECE diagnostic that includes the effect of suprathermal electrons is constructed: the YODA code.

2. Electron Cyclotron Emission in Tokamak Plasmas

Over the years, different ECE configurations were explored. The first was the LFS ECE. It is able to diagnose the electron temperature profile when the electrons are in thermal equilibrium. On the other hand if there are fast electrons in the bulk plasma and they emit towards the LFS, unfortunately they cross the EC cold resonance position, therefore everything one measure in the LFS ECE is the sum of the suprathermal emission plus the bulk emission. Another

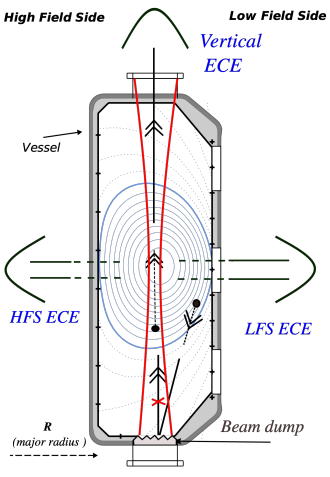

Figure 1: TCV ECE configurations [2]

idea was to use the HFS ECE because in that case the electrons do not encounter the cold resonance position, but it is impossible to assign an energy to the emission because there might be electrons at very different energies which emits at the same frequency along the same line of sight (LOS).

2.1. The Vertical ECE

To avoid these problems, the idea was to measure ECE at various frequencies along vertical LOSs (VECE) with constant magnetic field amplitude, providing a scan in electron energy via the relativistic factor γ because the VECE resonance reduces to $\omega \propto n/\gamma$, if the radius is fixed. The TCV Vertical ECE has an antenna with a line of sight tahat terminates with a Macror viewing dump characterized to absorb the 99.9% of the incident ECE radiation which falls on it. The EC radiation emitted in the plasma is collected by the collecting optics at the top of the machine where is also present a wire grid polarizer that allow to discriminate between the two polarizations of the EC radiation. After the splitting, the 2 polarized waves are transported through corrugated waveguides to the 4 Heterodyne radiometers, accurately setup in the ECE range. It allows simultaneous measurements of the same electron energy in different polarizations.

2.1.1 Mitigation of the BKG Radiation

The diagnostic limit is that specific plasma conditions are required for VECE measurements to detect only radiation originating from an isolated vertical volume in the tokamak, avoiding the so called *background radiation* (BKG). There are two main reasons why one must take care of the experimental conditions when this type of measurement is performed:

1. To avoid the cutoffs of the EC waves originating within the LOS;
2. The refraction phenomenon, inside the plasma volume, can change the direction and the shape of the VECE antenna pattern, which can for example miss the viewing dump.

The background polluting radiation was demonstrated to originate as thermal radiation near the cold resonance position of the EC 2^{nd} harmonic X-mode (X2) emission in TCV. Therefore the most efficient solution to clean the VECE

measurement was demonstrated to be leaving the X2 cold resonance position right outside the TCV vessel, by varying the magnetic field [2] as shown in figure 2.

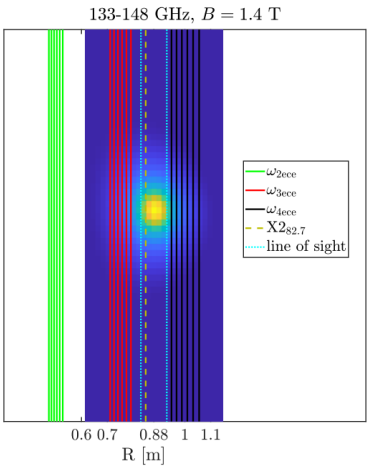

Figure 2: Radial location of the harmonics contributing to the background radiation for selected frequencies and magnetic field values.

In this thesis work, only TCV shots and VECE frequencies in which the refraction problem is avoided are exploited, allowing for more precise comparison between experimental measurements and simulations.

3. Modelling Tools & Methods

The VECE response to non-thermal electron population in the plasma is modelled by the new synthetic ECE YODA which calculates:

- the EC emission and (re)absorption based on any arbitrary numerical electron distribution function calculated by any first-principle kinetic code (as the 3D bounce-averaged relativistic Fokker-Planck code LUKE [5]) for arbitrary line of sight simulated using the C3PO ray-tracing code [6], which also model the detection system;
- the transport of EC radiated intensity along the propagation path.

YODA takes as inputs: ray-tracing quantities from C3PO, the numerical electron distribution function from LUKE and the magnetic equilibrium reconstructed by the LIUQE code. Then YODA re-elaborates these inputs, solves the integrals for the Electron Cyclotron absorption and emission and then with these quantities it solves the radiation transport equation to find the synthetic EC intensity at the antenna.

3.1. Modelling the EC Absorption and Emission

The *radiation transport equation* is a balance equation which describes how the energy carried by an EC wave can evolve in an inhomogeneous medium [1]. It depends on several quantities

- the *ray refractive index* $N_r(s)$, which distinguish itself from the plasma refractive index by the fact that the refractive index describes the ray trajectory along the wave vector $\boldsymbol{k}$, while the ray refractive index $\boldsymbol{N}$ is much related to the energy flux along the group velocity of the wave;
- The *spectral intensity* $I_\omega(s)$, a quantity that describes the power carried by the EC wave per unit of area, unit of solid angle and unit frequency;
- The EC *emissivity* $j_\omega(s)$ and the EC *absorption coefficient* $\alpha_\omega(s)$ which model the continuous EC absorption/emission processes along the ray path s in the plasma;

Calculating the $\alpha_\omega(s)$ and $j_\omega(s)$ integrals explicitly is then a necessary step to have an ECE synthetic diagnostic which accounts for any arbitrary numerical distribution function. To derive these integrals it is necessary to make the *weak damping approximation* and use the kinetic theory to describe this collisionsless resonant absorption and re-emission of electromagnetic waves [3]. These expressions are double integrals in the non-dimensional momentum space $(p_\parallel, p_\perp)$ normalized to the electron thermal momentum p_{Th}. These expressions take into account the wave polarization, the finiteness of the Larmor radius, the EC resonance condition and the electron distribution function. The presence of a resonance condition exploited by a Dirac delta into both the integrals, allows to reduce the them to 1D integrals over $p_\perp$. In this form, YODA calculates them numerically using an adaptive quadrature method. Having $\alpha_\omega(s)$ and $j_\omega(s)$, the radiation transport equation can be solved numerically by tracing back the rays from the dump to the antenna (where $I_\omega(s_{dump}) \sim 0$), by exploiting the reciprocity theorem on Maxwell's equations.

3.2. Mimicking the VECE Antenna Pattern

C3PO mimick the gaussian VECE antenna pattern in the WKB approximation (geometric op-

tics) allowing the ray-tracing approach, in which a radiation beam pattern is modelled by means of rays. Each ray in the pattern carries the same power in C3PO, therefore the guassian shape is obtained by construction. To calculate the antenna spectral intensity, it is then sufficient to solve the radiation transport equation for each ray, to sum all these quantities and then to divide this sum by the total number of the rays. Using a well diagnosed TCV shot (#73003) a good convergence can be reached for 24 rays in the antenna pattern, disposed in order to have 6 rays in each of the 4 given radial positions.

3.3. Fokker-Planck Equation Modelling

LUKE calculates the electron distribution function using the finite element method. In the Bounce-Averaged Fokker-Planck equation, the variation in time of the electron distribution function is described as the sum of at least 4 operators which acts on the distribution: a Coulomb collisional operator, a quasilinear radio-frequency operator [4], a Ohmic operator and a quasi-linear radial transport operator. LUKE takes as input a magnetic equilibrium from LIUQE and experimental data (electron density and temperature) and then solves the bounce-averaged Fokker-Planck equation. It is also important to say that LUKE runs using stationary calculations, or using dynamical calculations taking into account induction effects also. Then the distribution function is read by a specific module of YODA which interpolates it, renormalize it and at the end come out with a change of coordinate according to the formalism used in YODA.

4. Results

4.1. YODA thermal validation

The first step to assess the validity of YODA was to benchmark its calculations with the SPECE code, which is already validated for thermal plasmas, in TCV also.
A stationary simulation was performed for $t = 1.9\,\mathrm{s}$, using only 1 ray into the antenna pattern for the frequency range $113 - 118\,\mathrm{GHz}$. This solution is adopted since the simulation of only one ray in both SPECE and YODA allows for easier comparison between the results. For this ray, the X3 thermal resonances are simulated in both the codes and it resulted in a very good agreement between YODA and SPECE, as shown in figure 3. Such a good result, in force with the convergence of the antenna intensity for 24 rays in the antenna pattern mean that YODA gives reasonable results if it is used for thermal plasmas, with a complete antenna pattern.

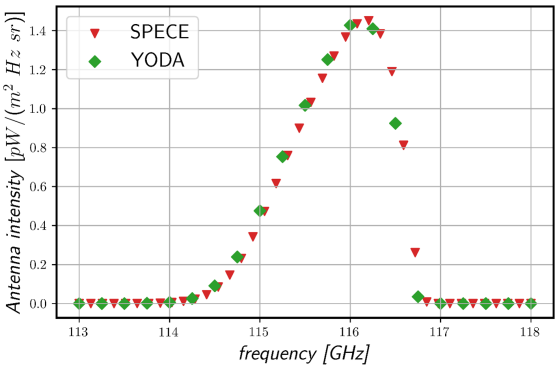

Figure 3: Comparison between YODA and SPECE spectral X-mode intensity calculations for $f \sim 113 - 118$ GHz (#73003 $t = 1.9$ s)

4.2. Scenario I

The TCV plasma discharge #73217 is an ECCD shot which has been specifically designed to achieve VECE measurements in which thermal and non-thermal EC emission can be observed separately during the shot [2]. The electron cyclotron heating phase occurs for about 1 second between $\sim 0.3\,\mathrm{s}$ and $\sim 1.3\,\mathrm{s}$ at a constant magnetic field of approximately $1.54\,\mathrm{T}$. The magnetic field strength is kept constant for approximately 100 ms after the heating is turned off until about $\sim$ 1.4s. The field is then ramped down from $1.54\,\mathrm{T}$ to $0.9\,\mathrm{T}$ for the remainder of the discharge. The heating phase takes place at a constant ECH power of around $500\,\mathrm{kW}$ and a constant launcher angle of approximately 10°. The launcher angle controls the direction of the ECH wave vector with respect to the toroidal magnetic field in the plasma. Perpendicular launching means that the ECH wave purely heats the plasma by increasing the perpendicular energy of the bulk electrons. Increasing the launcher angle allows the ECH wave to resonate with higher energy electrons and selected velocity parallel to the magnetic field, thereby driving a net toroidal current. In this discharge, the

plasma current is ramped down along with the magnetic field to maintain a quasi-frozen equilibrium [2]. This preserves the same X-mode polarization from the current drive to the calibration phase. A remarkable feature of this shot is the smooth ramp down of the magnetic field after $t \sim 1.4\,\mathrm{s}$, which allows for the identification of thermal peaks for each frequency. The thermal peak provides a self-calibration reference for the discharge #73217, using the value of the ECE synthetic power calculated at the thermal peak.

4.2.1 Simulations results

For the *scenario* I, to properly take into account the electric field response for a plasma current density variation in time, LUKE is set up to solve the drift kinetic equation using time dependent simulations and solving the induction equation. Fast electron radial transport is neglected (i.e. $D_r = 0\,\mathrm{m}^2/\mathrm{s}$) and the electron driven toroidal current calculated by LUKE, accounting for ECRH and Ohmic heating, matches the plasma current with less than 10% difference. In this simulation, also, a loss term for runaway electrons that is proportional to the ECRH power is included to account for the enhanced runaway electron transport observed in many recent experiment in the presence of ECRH. As shown in figure 4, simulations predict with good accuracy the VECE experimental trend during the steady ECH phase. Also, the VECE signal behaviour right after the heating is turned off is well matched. It means that in the $\sim 100\,\mathrm{ms}$ in which the ECH is turned off, while the magnetic field is left constant, the electron distribution function is predicted to come back to the Maxwellian distribution. It also confirms that all the measured EC emission in that case comes from suprathermal $\sim 60\,\mathrm{keV}$ electrons generated during the ECCD phase. On the other hand, it is clear that the synthetic VECE intensity is strongly underestimated during the heating onset. Further investigations are needed to understand the reasons why the models do not match the experimental trends in the initial phase.

4.3. Scenario II

In The TCV shot #72644, during the heating phase, the ECH power has a value similar to that of the hybrid discharge #73217, while the

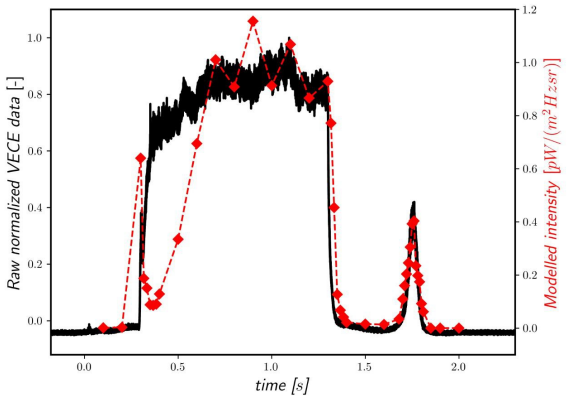

Figure 4: Comparison between synthetic VECE intensity trends and VECE raw data measured at 108.84 GHz in the #73217 disharge.

launcher angle is varied in 5 stationary steps between 0.7 s and 1.9 s. Here as well, the toroidal angle of the X2 launcher is kept constant at $\sim -90°$. The variation of the poloidal angle of the launcher from $\sim -10°$ to $\sim -26°$ in each stationary step leads to stair-shape X-mode intensities. When the heating is turned on at $\sim 0.7\,\mathrm{s}$, a sharp increase of the VECE signals is observed. This means that these measurements are not polluted by background radiation. At the ECH onset, only the higher frequency shows a sharp increase in measured intensity. The lower frequency also experiences a similar jump in intensity, but with a delay of over 500 ms, occurring only when the launcher angle is adjusted to its third stage.

4.3.1 Simulations results

The emphasis in the simulations of the #72644 VECE spectrum was placed in predicting the intensity jumps between the different steady state ECH phase and relate measurements to the density of fast electrons at selected frequencies. It is not necessary to do *time dependent* calculations in the kinetic simulation since the successive phases of constant ECH poloidal angle are sufficiently long to assume a quasi-steady state. Radial transport of fast electrons must be included to match the experimental plasma current during LUKE iterations. To stress the differences between the case in which the radial transport is taken into account and the one in which it is not accounted for two sets of simulations are carried out for two different ECE fre-

quencies: 108.84 GHz and 96.35 GHz. Both sets of simulations predict the step-like evolution of the VECE signal, with the $D_r = 0\,\mathrm{m}^2/\mathrm{s}$ simulation slightly overestimating the signal and the $D_r = 5\,\mathrm{m}^2/\mathrm{s}$ simulation slightly underestimating it, in both sets of frequencies. For the lower frequency - corresponding to the higher energy - the difference between the $D_r = 0\,\mathrm{m}^2/\mathrm{s}$ and the $D_r = 5\,\mathrm{m}^2/\mathrm{s}$ cases is more pronounced, with the $D_r = 5\,\mathrm{m}^2/\mathrm{s}$ case being sensibly closer to experimental measurements. With the better match of the toroidal current, this seems to indicate that radial transport of fast electrons indeed plays an important role.

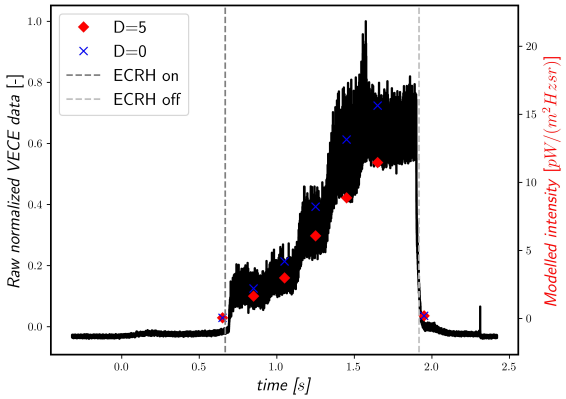

Figure 5: Comparison between synthetic VECE intensity trends for D$_r$ = 0 m^2/s and D=5 m^2/s cases and VECE raw data measured at 108.84 GHz in the #72644 disharge.

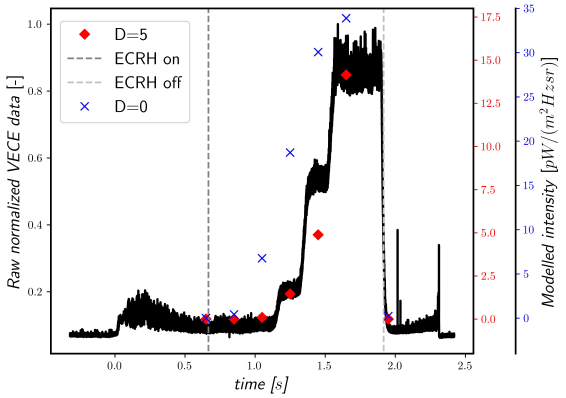

Figure 6: Comparison between synthetic VECE intensity trends for D=0 m^2/s and D=5 m^2/s cases and VECE raw data measured at 96.35 GHz in the #72644 disharge

5. Conclusion & Perspectives

The VECE detection system was successfully modeled through the use of the raytracing code C3PO. Also, it allows the simulation of any arbitrary line of sight, opening the possibility of using it not only for the vertical ECE, but also for low field side ECE and oblique ECE.
The YODA code was developed. It is a new general ECE synthetic diagnostic which accounts for any numerical arbitrary distribution function. YODA was first validated for thermal plasmas and then coupled with the 3D fully relativistic bounce-averaged Fokker-Planck code LUKE, allowing the reconstruction of ECE spectra in non-thermal electron scenarios. The VECE spectra of two TCV ECCD plasma scenarios (I : #73217 and II : #72644) were analyzed. For the first time, experimental VECE measurements were qualitatively compared with Fokker-Planck modeling (LUKE) coupled to the ECE synthetic diagnostic (YODA - C3PO) having promising results.

References

[1] G. Bekefi. *Radiation Processes in Plasmas*. John Wiley Sons, New York, 1966.

[2] A. Tema Biwole. *Measurement the electron energy distribution in tokamak plasmas from polarized electron cyclotron radiation*. PhD thesis, École Polytechnique Fédérale de Lausanne, 2023.

[3] M Bornatici and F. Engelmann. Electron cyclotron emission and absorption in fusion plasmas. *Nucl. Fusion*, 23:1153–1257, 1983.

[4] Dahye Choi. Experimental analysis of suprathermal electrons generated by electron cyclotron waves in tokamak plasmas. *Journal of Plasma Physics*, 86(2):905860201, 2020.

[5] J Decker and Y Peysson. Dke: A fast numerical solver for the 3d drift kinetic equation. EUR-CEA-FC-1736 EUR-CEA-FC-1736, Euratom-CEA, 2004.

[6] Y. Peysson and J. Decker. A versatile raytracing code for studying rf wave propagation in toroidal magnetized plasmas. *Plasma Phys. Control. Fusion*, 54(045003), 2012.